Expanded View Figures

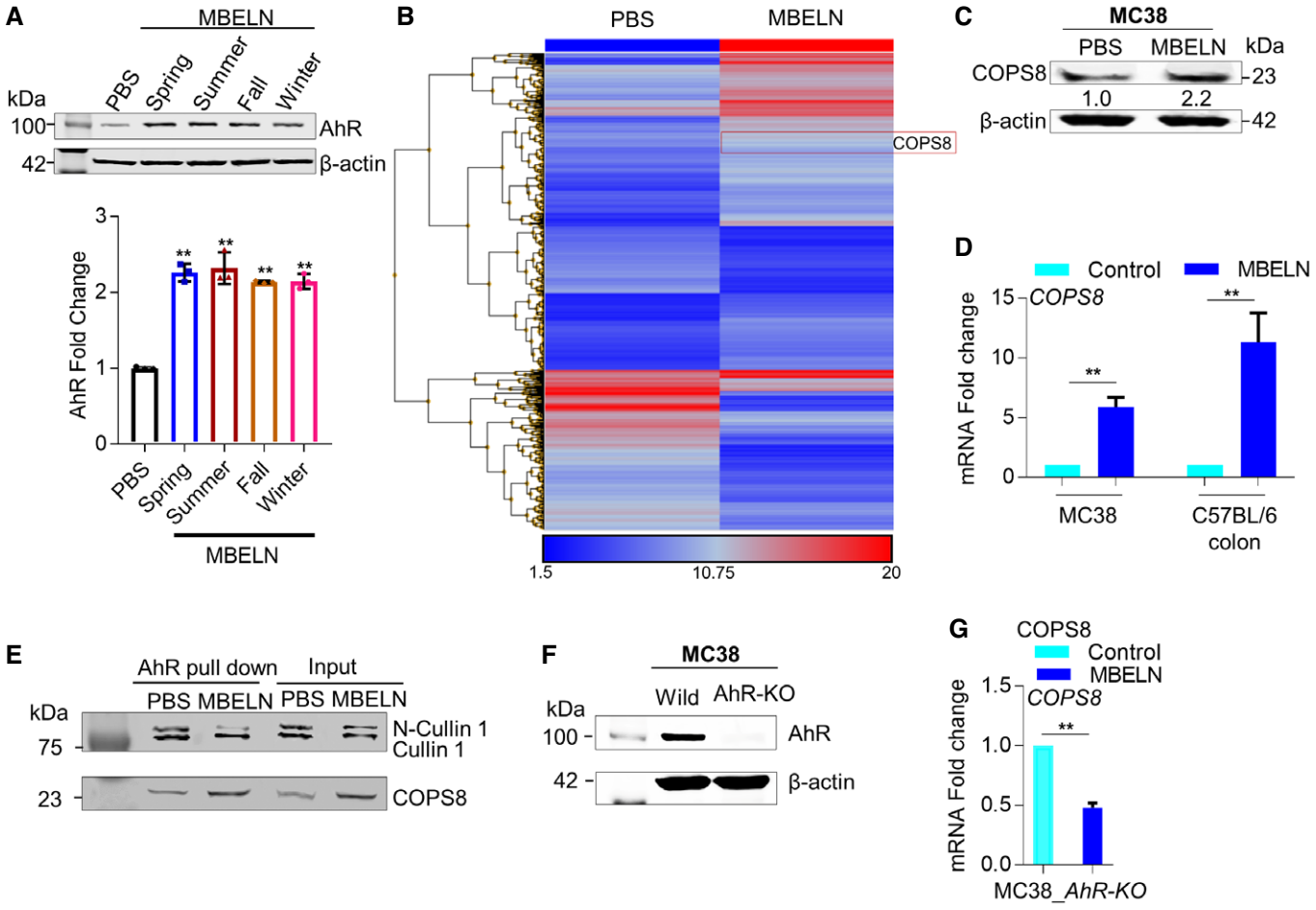

Figure EV1. MBELN-induced induction of AhR.

A To test the reproducibility of mulberry bark-derived exosome-like nanoparticles (MBELN) collected during different seasons of the year, MBELNs were extracted in spring, summer, fall, and winter and used to treat MC38 cells to evaluate AhR expression. Data are mean ± SEM from three biological replicates per group. $^{**}P < 0.01$ using one-way ANOVA.

B Heat map showing gene influences in crypts of villi in C57BL/6J mice. Data shown are from three technical replicates.

C Western blot for COP9/COP9 Constitutive Photomorphogenic Homolog Subunit 8 (COPS8) in MC38 cells following MBELN treatment. Data shown are from three biological replicates.

D mRNA expression of COPS8 in MC38 and after MBELN administration and C57BL/6J colon epithelial cells following MBELN administration for 7 days. Data are mean ± SEM from three biological replicates per group. $^{**}P < 0.01$ using Student's *t*-test.

E MC38 cells treated with MBELN and protein extract were immunoprecipitated using anti-aryl hydrocarbon receptors (AhR) antibody. The precipitate was subjected to Western blot with antibody against Cullin 1 (CUL1) and COPS8. Data shown are from three biological replicates.

F Western blot to confirm knockout of AhR in MC38 cells. Data shown are from three biological replicates.

G COPS8 mRNA expression in AhR-knockout (AhR-KO) MC38 cells following treatment with MBELNs. Data are mean ± SEM from three biological replicates per group. $^{**}P < 0.01$ using Student's *t*-test.

Source data are available online for this figure.

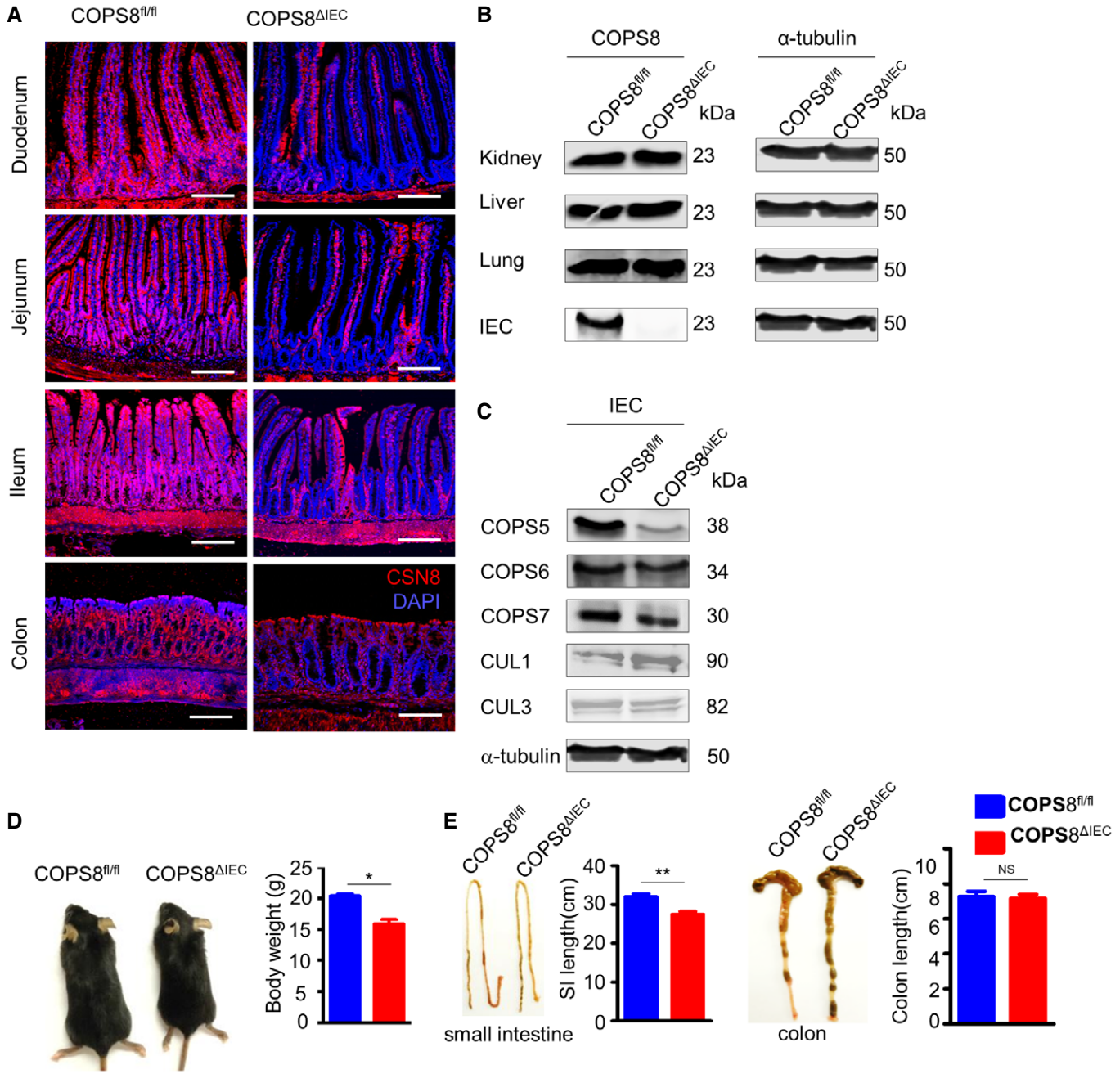

Figure EV2. Deletion of COP9/COP9 Constitutive Photomorphogenic Homolog Subunit 8 (COPS8) in intestinal epithelial cells (IEC) affects COP9 complex integrity.

A Immunofluorescence analysis of COPS8 protein expression with anti-COPS8 antibody (red) and with DAPI (blue) in the duodenum, jejunum, ileum, and colon from Villin-Cre and COPS8-lox alleles expressing (*COPS8*$^{fl/fl}$) and knockout *COPS8* in IEC (*COPS8*$^{\Delta IEC}$) mice. Scale bar, 100 μm, data are represented from seven biological replicates per genotype.

B, C Immunoblot analysis of COPS8 protein expression in the liver, kidney, lung, and IECs isolated from ileum of *COPS8*$^{fl/fl}$ and *COPS8*$^{\Delta IEC}$ mice and analysis of the associated proteins (COPS5, COPS6, COPS7, Cullin (CUL) 1 and 3) in lysates prepared from isolated IECs from *COPS8*$^{fl/fl}$ and *COPS8*$^{\Delta IEC}$ mice. Data are represented from seven biological replicates per genotype.

D Body size (representative pictures, left) and weight (right) of *COPS8*$^{fl/fl}$ and *COPS8*$^{\Delta IEC}$ mice at 4 weeks of age. Data are represented as mean ± SEM from seven biological replicates per genotype. *$P < 0.05$, NS—non-significant using Student's *t*-test.

E Length of small intestine and colon from *COPS8*$^{fl/fl}$ and *COPS8*$^{\Delta IEC}$ mice. Data are represented as mean ± SEM from seven biological replicates per genotype. **$P < 0.01$, NS—non-significant using Student's *t*-test.

Source data are available online for this figure.

Figure EV3. Paneth cell loss in *COPS8*$^{\Delta IEC}$ mice.

A Representative hematoxylin and eosin (HE) staining of duodenum and jejunum showing loss of Paneth cells (black arrow) in *COPS8*$^{\Delta IEC}$ mice. Scale bar 50 μm, data are represented from seven biological replicates per genotype.

B The granule protein, lysozyme, was examined by immunofluorescence (Red) and counted in the duodenum and jejunum (located above dashed line) of Villin-Cre and COPS8-lox alleles expressing (*COPS8*$^{fl/fl}$) and *COPS8*$^{\Delta IEC}$ mice. Scale bar 200 μm. Data are represented as mean ± SEM from seven biological replicates per genotype. $^{**}P < 0.01$ using Student's *t*-test.

C Transmission electron microscopy (TEM) of crypts of *COPS8*$^{fl/fl}$ and *COPS8*$^{\Delta IEC}$ mice. The base of the crypt in *COPS8*$^{\Delta IEC}$ mice is occupied by poorly differentiated columnar epithelial cells that lack secretory granules, rudimentary electron-dense granules (black arrows), microvilli (yellow arrows), and granules in the lumen (blue arrows). Scale bar 5 μm.

D Goblet cells from *COPS8*$^{fl/fl}$ and *COPS8*$^{\Delta IEC}$ mice were stained with Alcian blue and counted in the ileum. Scale bar 50 μm. Data are represented as mean ± SEM from seven biological replicates per genotype. NS—statistically non-significant using Student's *t*-test.

E The marker for enteroendocrine cells, chromogranin, was detected by immunofluorescence and counted in the duodenum and jejunum of *COPS8*$^{fl/fl}$ and *COPS8*$^{\Delta IEC}$ mice. Scale bar 100 μm. Data are represented as mean ± SEM from seven biological replicates per genotype. $^{**}P < 0.01$ using, NS—non-significant using Student's *t*-test.

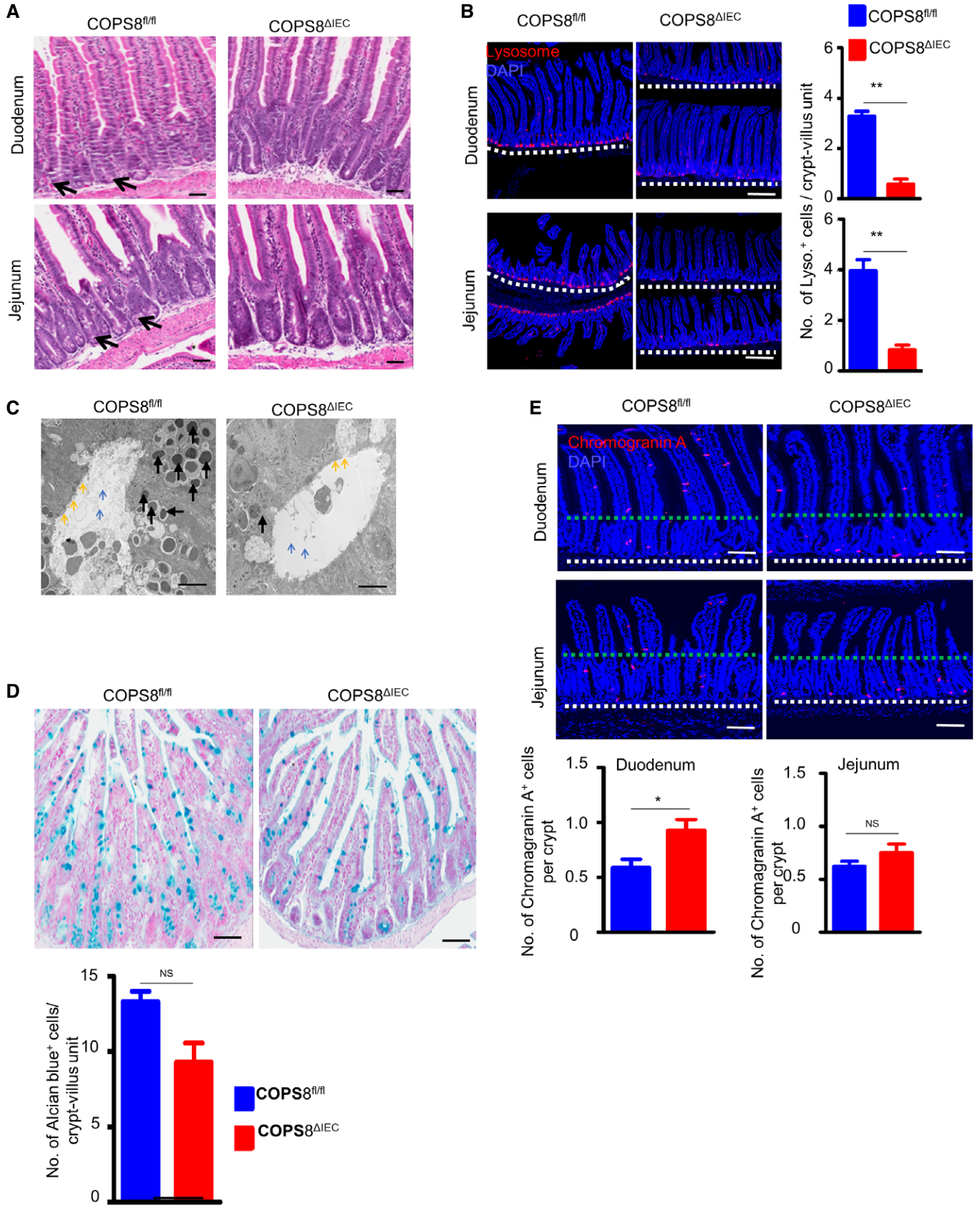
A
COPS8fl/fl
COPS8ΔIEC
Duodenum
Jejunum
B
COPS8fl/fl
COPS8ΔIEC
Lysosome
DAPI
Duodenum
Jejunum
COPS8fl/fl
COPS8ΔIEC
No. of Lyso.+ cells / crypt-villus unit
**
**
C
COPS8fl/fl
COPS8ΔIEC
D
COPS8fl/fl
COPS8ΔIEC
NS
No. of Alcian blue+ cells/ crypt-villus unit
COPS8fl/fl
COPS8ΔIEC
E
COPS8fl/fl
COPS8ΔIEC
Chromogranin A
DAPI
Duodenum
Jejunum
No. of Chromagranin A+ cells per crypt
Duodenum
*
No. of Chromagranin A+ cells per crypt
Jejunum
NS

Figure EV3.

Figure EV4. Deficiency of COP9/COP9 Constitutive Photomorphogenic Homolog Subunit 8 (COPS8) increases susceptibility to dextran sodium sulfate (DSS)-induced colitis.

A, B Representative image of histological analysis of the distal ileum of *COPS8*$^{fl/fl}$ and *COPS8*$^{\Delta IEC}$ mice by hematoxylin and eosin (HE) staining (A) and column graph (B) showing cellularity (severity score) in the lamina propria. Scale bar 100 μm. Data are represented as mean ± SEM from seven biological replicates per genotype. *$P < 0.05$ using Student's *t*-test.

C Production of proinflammatory cytokines interleukin (IL)-1β, IL-6 and tumor necrosis factor-α (TNF-α) in intestinal epithelial cells (IEC) of *COPS8*$^{fl/fl}$ and *COPS8*$^{\Delta IEC}$ mice. Data are represented as mean ± SEM from seven biological replicates per genotype. *$P < 0.05$ using Student's *t*-test.

D Neutrophils, CD11b^{+}-Ly6C^{+} (upper panel) and CD11b^{+}-Ly6G^{+} (lower panel), infiltration in colonic lamina propria of *COPS8*$^{fl/fl}$ and *COPS8*$^{\Delta IEC}$ mice. Column graph showing percentage of neutrophils CD11b^{+}-Ly6C^{+} and CD11b^{+}-Ly6G^{+} presented as mean ± SEM from seven biological replicates per genotype. *$P < 0.05$, NS—non-significant using Student's *t*-test.

E Percentage of Treg cells (upper panel) and ratio of Th1/Th17 cells (lower panel) colonic lamina propria of *COPS8*$^{fl/fl}$ and *COPS8*$^{\Delta IEC}$ mice. Data are represented as mean ± SEM from three biological replicates per genotype. *$P < 0.05$, NS—non-significant using Student's *t*-test.

F Western blot for nuclear factor kappa B (NF-κB) in Villin-Cre and COPS8-lox alleles expressing (*COPS8*$^{fl/fl}$) and IEC *COPS8* knockout (*COPS8*$^{\Delta IEC}$) mice colon tissue following treatment with phosphate-buffered saline (PBS), DSS and DSS with mulberry bark-derived exosome-like nanoparticles (MBELNs). Data are mean ± SEM. *$P < 0.05$, using Student's *t*-test and one-way ANOVA.

Source data are available online for this figure.

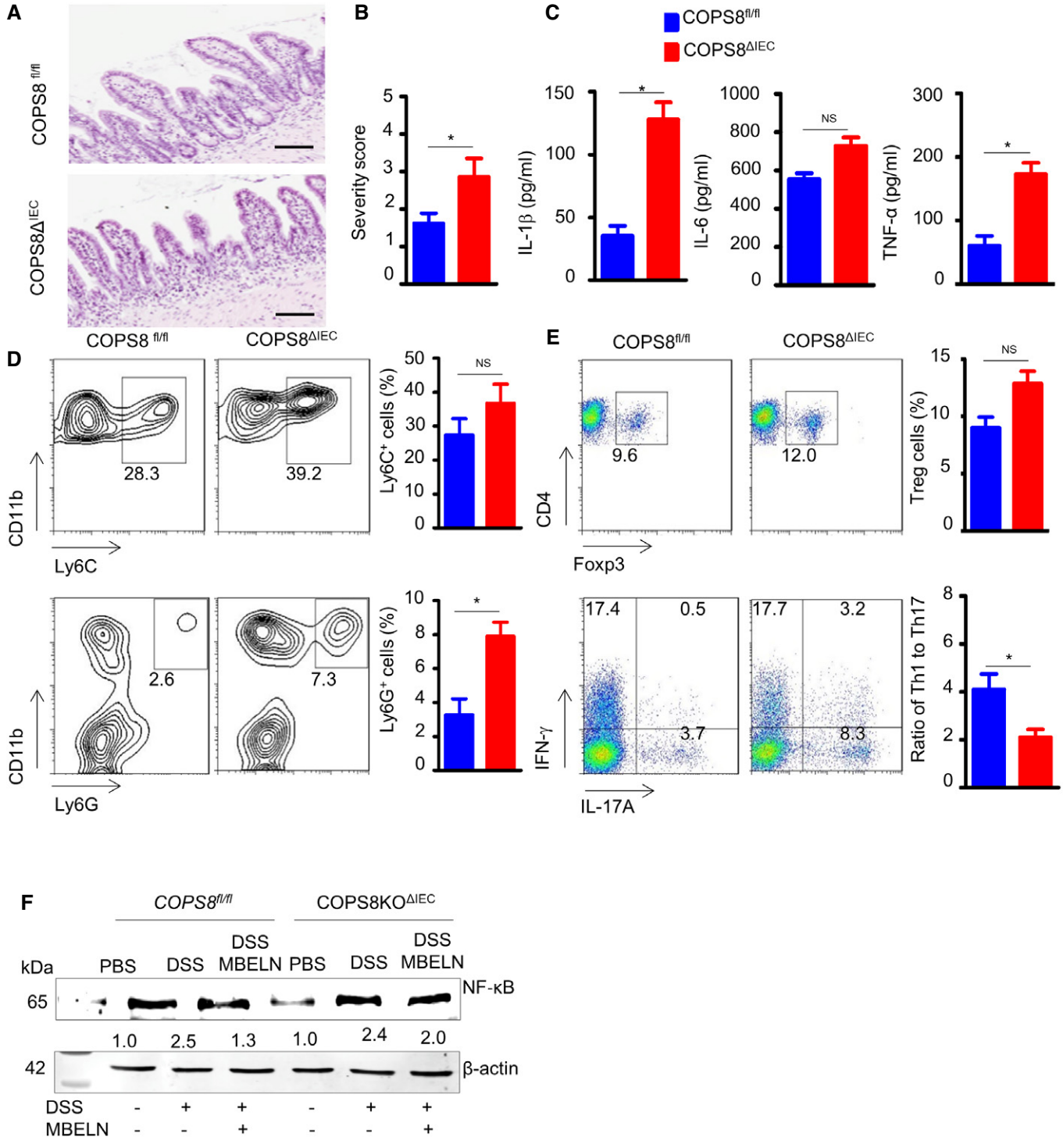
A
COPS8 fl/fl
COPS8ΔIEC
B
Severity score
C
COPS8fl/fl
COPS8ΔIEC
IL-1β (pg/ml)
IL-6 (pg/ml)
TNF-α (pg/ml)
NS
D
CD11b
Ly6C
28.3
39.2
Ly6C+ cells (%)
Ly6G
2.6
7.3
Ly6G+ cells (%)
E
CD4
Foxp3
9.6
12.0
Treg cells (%)
IFN-γ
IL-17A
17.4
0.5
3.7
17.7
3.2
8.3
Ratio of Th1 to Th17
F
COPS8fl/fl
COPS8KOΔIEC
kDa
PBS
DSS
DSS MBELN
NF-κB
65
1.0
2.5
1.3
2.4
2.0
β-actin
42
DSS
MBELN

Figure EV4.

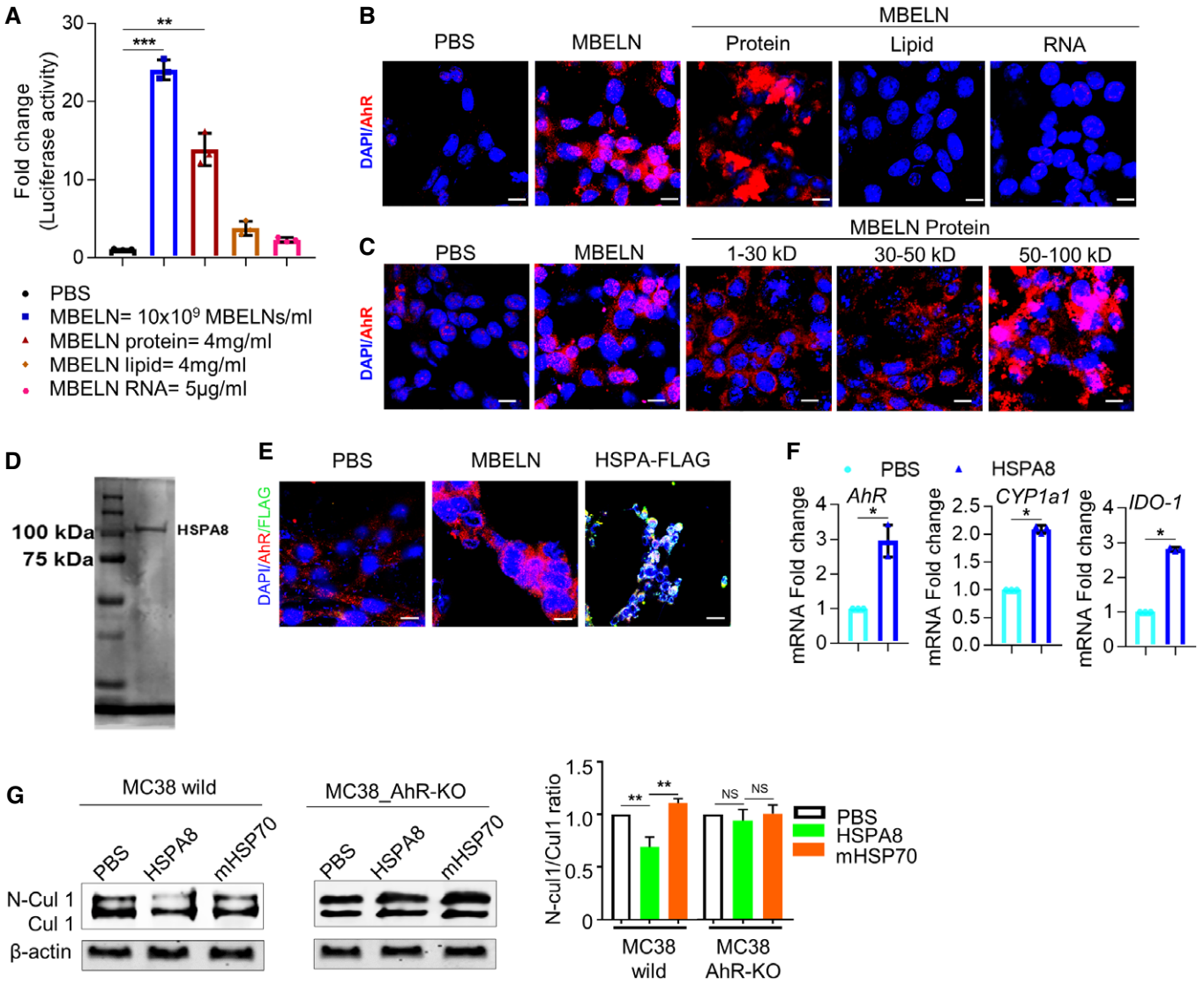

Figure EV5. Analysis of the MBELN factor (protein, lipid, and RNA) liable for AhR induction.

A Effect of different fractions of mulberry bark-derived exosome-like nanoparticles (MBELNs) on the expression of aryl hydrocarbon receptor (AhR) promoter using HEPA1.1 cells (AhR responsive luciferase reporter construct). Data are represented as mean ± SEM from three biological replicates. *$P < 0.05$, NS—non-significant using one-way ANOVA.

B Confocal image showing the effect of MBELN fractions on localization of AhR. Scale bar 10 µm, Data are represented from three biological replicates.

C The effect of different molecular weight fractions of MBELN-derived proteins on AhR localization in MC38 cells. Scale bar 10 µm, Data are represented from three biological replicates.

D Cloning, expression, and purification of recombinant MBELN-HSPA8.

E Confocal microscopy showing FLAG-tagged HSPA8 protein treatment to MC38 colocalized with AhR. Scale bar 10 µm, Data are represented from three biological replicates.

F Real-time quantitative reverse transcription polymerase chain reaction (PCR) for expression of AhR and its targeted genes Cytochrome P450, family 1, subfamily A, polypeptide 1 (CYP1a1), and Indoleamine 2,3-dioxygenase (IDO-1) in MC38 cells following HSPA8 treatment. Data are represented as mean ± SEM from three biological replicates. *$P < 0.05$ using Student's *t*-test.

G Western blot showing the ratio of CUL1 and neddylated cullin 1 (N-CUL1) expression in wild and AhR knockout (KO) MC38 cells. Data are represented as mean ± SEM from three biological replicates. *$P < 0.05$, NS—non-significant using Student's *t*-test.

Source data are available online for this figure.